New Avenues in Confocal Surface Plasmon Microscopy

Michael G. Somekh, Suejit Pechprasarn, Wai-Kin Chow, Jingkai Meng, Hong Shen
Department of Electronic and Information Engineering,
The Hong Kong Polytechnic University,
Kowloon,
Hong Kong

ABSTRACT

The principal strength of the confocal microscope for biological imaging lies its ability to detect only light that emerges at close to the focal plane, eliminating light originating from different focal planes. We discuss how this confocal property has considerable advantage in the detection of surface plasmons, since it defines the path of the detected radiation, thus greatly improving the lateral resolution and also the measurement precision. In this paper we show how a spatial light modulator in the back focal plane allows one to generate a whole range of new imaging properties that confer great flexibility on the system. The technique allows one to measure surface wave velocity, surface wave attenuation and perform rapid single shot measurement and effect common path operation.

1. INTRODUCTION

Surface plasmons (SPs) are surface waves confined to the interface between a metal with negative permittivity, such as gold, and a dielectric. There are several ways to excite SPs and of most relevance to the present paper is the so-called Kretschmann-Raether configuration, where light is incident from a region of high index to a metal film of typical thickness around 50nm and a dielectric region which constitutes the analyte whose average index will be lower than the top region, this simple situation is depicted in figure 1.

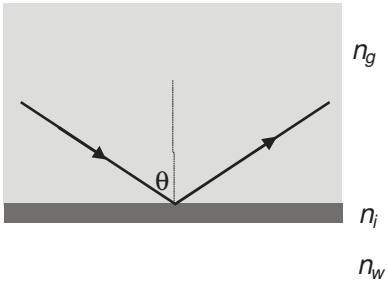

Figure 1 Simple three layer structure for excitation of surface plasmons. Top layer, n_g, is a higher index layer which carries the incident radiation, n_i is the metal (gold) used to support the plasmons and n_w is the final layer where the sensing takes place.

Excitation of SPs occurs when the incident *k*-vector matches the real part of the *k*-vector of the SPs. This is manifested in a dip in the reflectivity close to the incident angles where the *k*-vectors match, since in this case energy is coupled into the SPs some of which is dissipated due to ohmic losses. This is very easily observed, less easy to observe is the phase change that is associated with the excitation and reradiation of the SP. This phase change is, in fact, a more general property compared to the dip in the reflectivity, since, unlike the dip, it occurs when surface waves are excited on material and systems with no loss such as dielectrics.

The reason that SPs are so useful for biological measurements is that the value of the *k*-vector of the SP is highly dependent on the ambient medium, n_w. For this reason SPs are widely used for detection of small amounts of analyte, for

Plasmonics in Biology and Medicine XIII, edited by Tuan Vo-Dinh, Joseph R. Lakowicz, Ho-Pui A. Ho, Krishanu Ray,
Proc. of SPIE Vol. 9724, 972409 · © 2016 SPIE · CCC code: 0277-786X/16/$18 · doi: 10.1117/12.2223223

instance, antigen/antibody binding reactions [1]. The problem with SPs and surface waves in general is that, as the name, suggests they travel along the sample, indeed the sensitivity of SP sensors improves with the sharpness of the resonance curve, which, in turn, is related to the propagation distance of the SPs [2]. A long propagation length means that detection of multiple analytes which are closely spaced is very challenging since there will be a great deal of crosstalk between adjacent measurement locations. This means that, in effect, there is trade-off between sensitivity and resolution.

The confocal microscope is commonly used in biological imaging to extract information from the focal plane eliminating light that does not appear to come from the focus. This very property is also extremely useful when trying to localize SP measurements. This can be seen in figure 2 below which shows a stylized representation, with the excitation path omitted, of a confocal microscope used to excite and detect SPs.

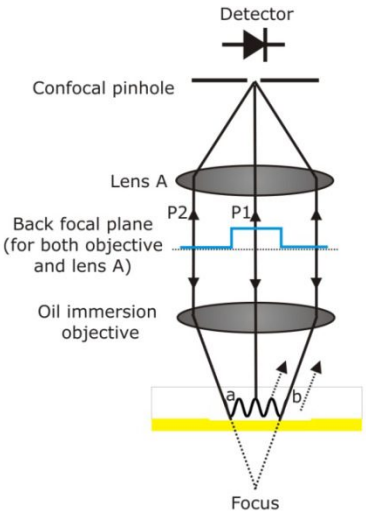

Figure 2 Simplified diagram of confocal microscope used to excite a SP. Note that the SP appears to be excited at point 'a' and reradiated at 'b'

We can see from figure 2 that the oil immersion lens provides the high index medium, n_g, required to excite the SPs. Consider a wave excited at 'a', this will reradiate continuously along the surface shedding energy as it propagates. For a typical prism based system or a non-confocal system all the reradiating light can be detected. In the confocal system the very property that allows one to eliminate light from out of the focal plane will also ensures that light detected has travelled through a well-defined path. The system thus ensures that the path length of the propagating SPs is defined by the properties of the optical system rather than the properties of the SPs themselves. This is the basis for the application of the confocal microscope for SP measurement. In addition, we add a spatial light modulator (SLM) conjugate to the back focal plane (BFP) which adds enormous versatility to the available processing options [3]. SLMs are also becoming very widely used in other forms of microscopy [4] for precisely the same reasons as in our work: they confer great flexibility within a single hardware platform.

2. EMBEDDED INTERFEROMETRY

If we look at figure 2 again we can see that there are two principal paths that return to the detection pinhole, P2 is the path involving the SP as discussed in the introduction, while P1 represents a path close to normal incidence which also returns to the detector. These paths in effect form an interferometer, which we term 'embedded' simply because both paths are locked into the same system. As the sample is defocused we observe the so-called *V(z)* effect where the P1 and P2 interfere. Examples of such curves are shown in figure 3. These show how the period of the ripple changes with material properties and also how the interference effect becomes less distinct when the size of the pinhole increases. This is because light arrives at the detection plane from different paths and the phase corresponding to these paths differs resulting in phase cancellation. In practice, there is no physical pinhole in the back focal plane, so that the CMOS

camera, detects the light returning to the image plane and the effective pinhole size is controlled simply by choosing the number of pixels used to recover the signal.

The period of the ripple, Δz, for the ideal confocal system is given by:

$$\Delta z = \frac{\lambda}{2n_g(1-\cos\theta_p)} \qquad (1)$$

Where θ_p is the angle for excitation of SPs.

θ_p gives a direct measure of the wavevector of the SP as given in equation 2.

$$k_p = \frac{4\pi n_g}{\lambda}\sin\theta_p \qquad (2)$$

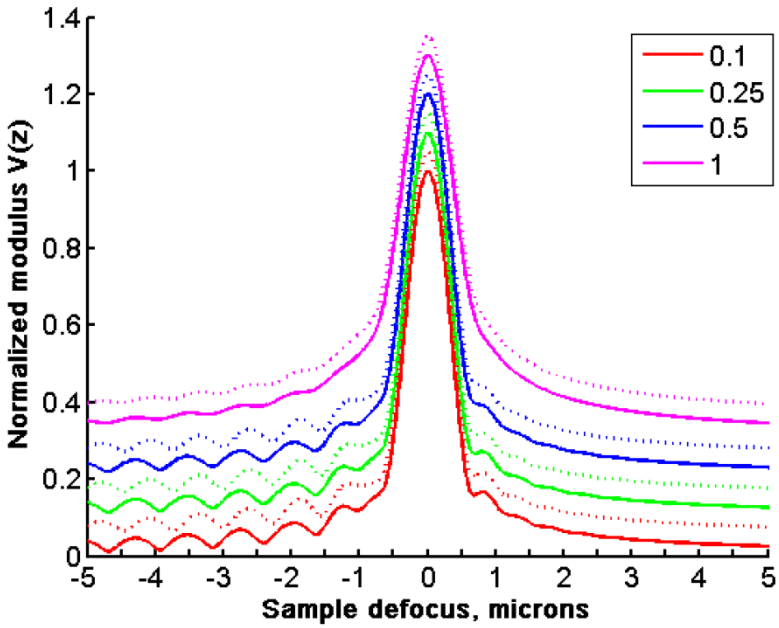

Figure 3 Simulated *V(z)* curves for different pinhole diameters. Solid curves 50nm bare gold, dashed curves gold with 10nm overlayer with refractive index 1.5. Each pinhole is displaced by 0.1units on the y-axis and curves corresponding to the overlayers are displaced by a further 0.05 on the y-axis. Pinhole radii are defined in terms of Airy disc radius (0.61λ/NA) are shown on the legend. Reprinted with permission from Optics Express

In our earlier work the sample was physically defocused but more recently we simply perform the defocus by imposing the appropriate phase distribution to the SLM [5].

The SLM provides many other benefits. For instance, we can make far more accurate measurements by realizing that we can use the SLM to change the phase of the reference beam relative to the sample beam and apply a phase stepping algorithm, so that the phase of the SP can be extracted directly. In essence, we are phase stepping P1 relative to P2 and extracting their relative phase. The phase difference, ϕ, between these two components varies as: $\phi(z) = \frac{4\pi n_g}{\lambda}(1-\cos\theta_p)z + \text{constant}.$ A plot of phase difference between reference and SP component (in the appropriate region of negative defocus) therefore gives a line whose gradient is given by:

$$\frac{d\phi}{dz} = \frac{4\pi n_g}{\lambda}\left(1-\cos\theta_p\right) \qquad (3)$$

This approach is provides an accurate and reliable method to measure the SP and measurement of the gradient of the phase is more reliable compared to measurement of the period of an oscillation which is the case when the *V*(z) period is measured directly. Figure 4 shows the gradients obtained for bare gold and a gold layer coated with indium tin oxide (ITO) deposited onto a gold surface. The thickness of the ITO was measured with an ellipsometer by illuminating the sample from the coating side, the thickness value obtained was 11nm±2.3nm. We can also determine the properties of the coating from the gradient of ϕ with respect to defocus, z, using the SP microscope imaging through the gold. Using a refractive index of 1.86, we can recover a thickness of 13.4nm which is in quite good agreement [6]. In this case, of course, illumination was through the gold layer, which is much more useful for biological measurements since the optical beam does not pass through the region where the biological processes are taking place, in other words, the measurement system and the measurand are well separated.

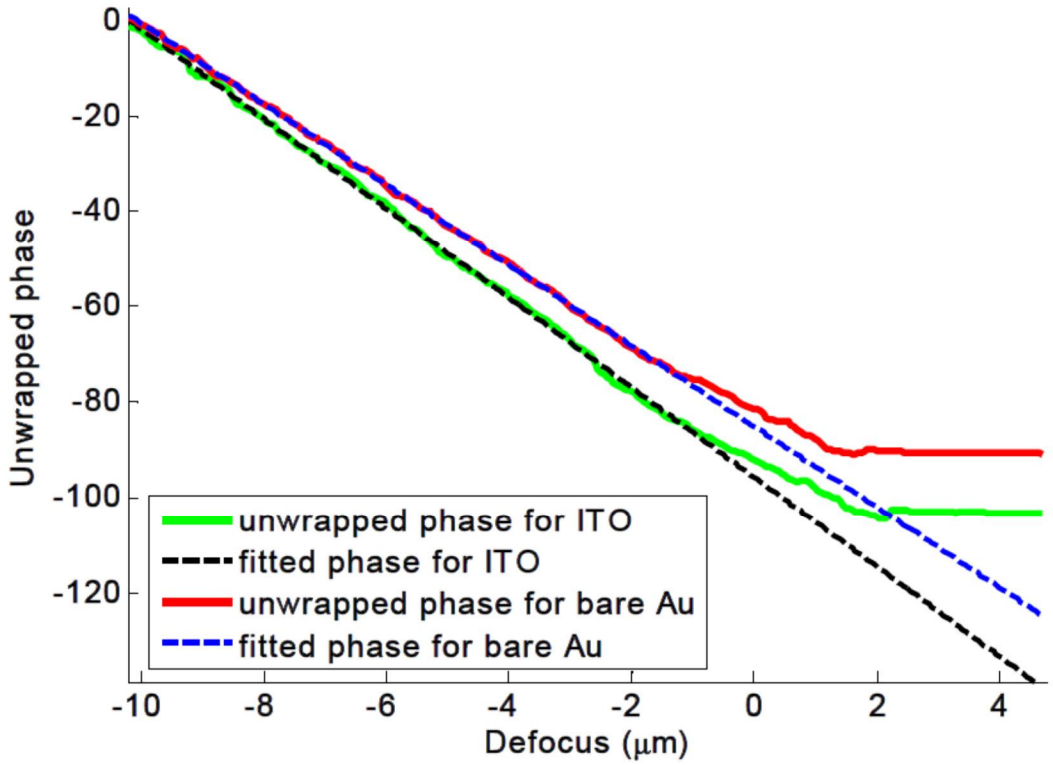

Figure 4 Experimental $\phi(z)$ obtained applying a phase stepping algorithm to four $V(z)$ curves. The red curve fits the values for the bare gold and the blue curve fits the ITO coated gold; the dashed lines are the linear fits.

The idea of embedded interferometry and is extremely powerful and allows one to ensure the sample and reference beam are incident at the same angle. Using linear polarization on the back focal plane there is a continuous variation between incident TE polarization, which does not produce a SP and TM polarization that excites a SP. Referring back to figure 1, the path that returns to the pinhole requires the incident light to be converted to a surface wave, otherwise, it would be reflected at the point of incidence and miss the pinhole. If, however, we impose a phase gradient on the back focal plane which deflects the incident beam so that it hits point 'b' of figure 1 rather than point 'a', then it will be reflected so that it passes into the pinhole. By allowing the region of predominant TM polarization to hit the sample without any additional phase gradients and forcing the azimuthal angles with predominant TE polarization to bend the incident beam, we are

able to force the incident TE and TM beams to interfere. The reference beam and the probe beam are now incident at the same angle of incidence, so that any phase noise due to microphonics introduced on one beam will be common to both and thus cancel. We have demonstrated the robustness of this approach by deliberately inducing noise on the optical table and the common path system was extremely stable while the system with a normal incident beam was unable to reconstruct a reliable value of θ_p [7]

3. EMBEDDED INTERFEROMETRY WITH VORTEX BEAMS

The interferometers described in the previous sections allow the SP wavevector to be measured relatively easily, however, the drawback of these systems is that it is necessary to perform several phase steps to recover the phase. This is often not a problem but it does limit the speed of measurement because the SLM used needs approximately 500ms to switch states, so in situations where measurement speed is critical we would like to reduce the number of phase steps. A single shot interferometer will mean that it is only necessary to switch the SLM when we wish to change the defocus.

In order to perform single shot measurement it is necessary to have a reference beam that has a range of different phases so that the phase stepping algorithm can be recovered in a single measurement. This may be achieved using a reference beam with an azimuthal phase variation at the angles corresponding to low incident angles. This is shown schematically in figure 5.

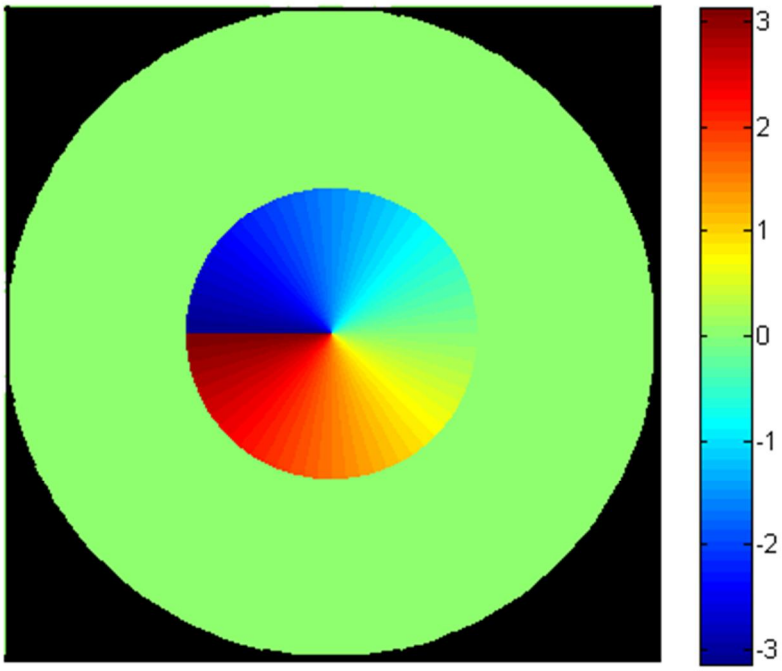

Figure 5. Phase distribution applied in the back focal plane for single shot embedded interferometry. The regions corresponding to the reference beam have an axial phase variation, whereas the angles that excited the SPs have no additional phase profile.

The azimuthal phase variation means that the reference beam on the sample (and the image projected to the detector) is a vortex beam with zero amplitude in the center. The donut beam has an azimuthal phase variation similar to the phase variation in the excitation plane. Now rather than using a single reference point in the center of the image plane we

choose four points at symmetrical axial positions, each giving a different phase shift for the reference beam. These different phase shifted reference signals, provide the signals required to recover the phase of the SP. The signal at these four points provide the signals to input into a phase stepping algorithm to recover the phase of the SP relative to the reference. This single shot approach has been compared with results obtained using normal incidence reference beam with very similar results. These are tabulated in the table below.

	Vortex		Phase Step	
	θ°	recovered t [nm]	θ°	recovered t [nm]
Bare Au	44.06	-	44.06	-
Layer 1	45.38	5.72	45.31	5.46
Layer 2	46.62	9.77	46.59	9.67
Layer 3	48.62	14.70	48.37	14.16

Table 1 Comparison between phase stepping measurements obtained with four *V(z)* measurements and vortex measurement obtained from a single measurement with the phase steps extracted from four points.

These show measurements were taken on bare gold and three additional layers of added ITO. The table shows that recovered values of film thickness using the single shot and the four phase steps agree very well, these, in turn, agree well with independent surface profile measurements.

4. BEYOND SIMPLE DEFOCUS

We mentioned in section 2 that the SLM is used perform electronic defocusing by imposing a phase shift distribution on the back focal plane that corresponds to the phase shifts that would be imposed by a physical defocus. For instance, the phase shift on the back focal plane necessary to represent a defocus Δz is given by:

$$\frac{4\pi n_g}{\lambda}\cos\theta\,\Delta z \tag{4}$$

Where θ is the incident angle whose sine is proportional to the radial position in the back focal plane. Although this is a very useful distribution for our purposes it has one major drawback. If we refer to figure 1 again we can see that the beam P1 which does indeed return to the pinhole is not in reality a single beam but consists of a small range of angles, so as the sample is defocused this beam diverges. This means that the signal from the path P1 that reaches the pinhole decreases with defocus. The effect of this is that the reference beam decreases with defocus so that the overall interference signal which is proportional to the product of the amplitude corresponding to the SP and the amplitude of the reference beam decreases greatly thus degrading the signal to noise ratio and restricting the range of defocuses for which the measurement may be used. We therefore modify the phase profile so that the phase corresponding to the reference beam with constant phase and the beam corresponding to the SP is curved so that is propagates between the points 'a' and 'b' of figure 1.

We therefore modify the phase variation so that it is given by:

$$\begin{aligned} &0 \text{ for } \theta \le \theta_0 \\ &\frac{4\pi n_g}{\lambda}\left(\cos\theta - \cos\theta_0\right)\Delta z \text{ for } \theta > \theta_0 \end{aligned} \tag{5}$$

Where θ_0 represents the edge of the reference region.

We shall report detailed quantification of this effect in a future publication but the effect is perhaps illustrated most graphically with the protein binding curves obtained with a decreasing reference beam due to phase curvature in the back focal plane and a reference beam with uniform phase. We can see that even at the reduced power used in this experiment to degrade the signal to noise ratio the phase distribution with the flat phase region give far better signal to noise ratio.

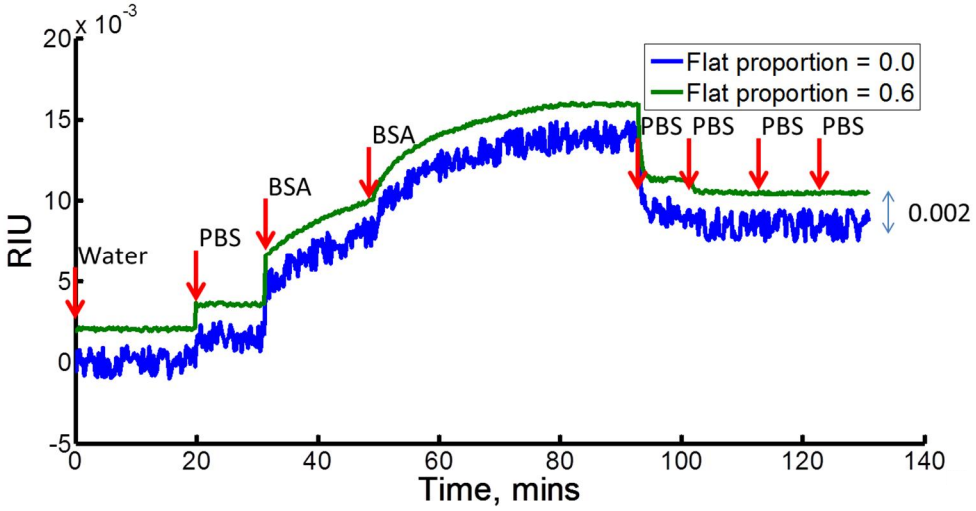

Figure 6 Non-specific binding of BSA to a gold substrate. Blue curve is for conventional measurement with curved reference beam, the green curve shows the same curve with a flat top occupying 60% of the back focal plane.

5 CONCLUSIONS

This paper has discussed different implementations of confocal surface plasmon interferometry. The confocal arrangement allows one to define the path of the surface waves rather than rely on their intrinsic decay. We do not, of course, change the propagation length of the SPs but do ensure that the detected light has emerged from a very well controlled path. This means that far denser arrays of sensing elements can be constructed without the effects of crosstalk. Although we have not discussed here the well-defined path means that the method is also very effective for the measurement of attenuation of surface waves.

The use of an SLM conjugate to the back focal plane means that we can construct many different types of interferometer such as phase stepping, common path and single shot interferometer. The advantage of the SLM is that it can be used to form beam profiles where different portions of the beam focus to different positions, this has been discussed in section 4 as a means to improve the signal to noise ratio. This approach can also be adapted for other forms of microscopy where focussing different parts of the angular spectrum into different planes will enable new imaging modes.

To conclude by combining the confocal microscope with SLMs there is enormous potential to make microscopic biosensors that can be optimized to measure different parameters such as the real part of the *k*-vector or the attenuation and also optimized against different performance parameters such as speed, signal to noise ratio or immunity to external noise. The real beauty of these optimizations is that they can all be achieved in the same hardware configuration and simply reprogrammed by changing the SLM settings.

6 REFERENCES

[1] Schasfoort R.B.M. and Tudos A.J.,[Handbook of Surface Plasmon Resonance], RSC Publishing, Cambridge (2008).

[2] Somekh M.G., "Surface plasmon and surface wave microscopy", in: P. Török, F.-J. Kao (Eds.), [Optical Imaging and Microscopy], Springer, Berlin, Germany, (2007).

[3] Zhang B., Pechprasarn S., Zhang J., and Somekh M., "Confocal surface plasmon microscopy with pupil function engineering," Opt. Express 20, 7388-7397 (2012).

[4] Maurer, C., Jesacher A., Bernet S., and Ritsch-Marte M., "What spatial light modulators can do for optical microscopy," Laser & Photonics Reviews, 5(1), 81-101 (2011).

[5] Zhang B., Pechprasarn S., and Somekh M., "Surface plasmon microscopic sensing with beam profile modulation," Opt. Express 20, 28039-28048 (2012).

[6] Zhang B.,Pechprasarn S., and Somekh M., "Quantitative plasmonic measurements using embedded phase stepping confocal interferometry," Opt. Express 21, 11523-11535 (2013).

[7] Pechprasarn S., Zhang B., Albutt D., Zhang J., and Somekh M.,"Ultrastable embedded surface plasmon confocal interferometry", Light: Science & Applications **3**, e187; doi:10.1038/lsa.2014.68 (2014)